

1 **Multimodal Sensorimotor System in Unicellular Zoospores of a Fungus**

2

3 Andrew J.M. Swafford¹ and Todd H. Oakley¹

4

5 ¹University of California Santa Barbara. Santa Barbara, California, 93106, USA.

6

7 **Running Title:** Multisensory System in Fungus Zoospores

8

9 **Corresponding author:** Todd Oakley - oakley@lifesci.ucsb.edu

10

11 **Keywords:** multisensory, zoospore, phototaxis, chemotaxis, allomyces, fungus

12

13 **Summary Statement:** Zoospores' ability to detect light or chemical gradients varies within
14 *Allomyces*. Here, we report a multimodal sensory system controlling behavior in a fungus, and
15 previously unknown variation in zoospore sensory suites.

17 **Abstract**

18 Complex sensory suites often underlie critical behaviors, including avoiding predators or
19 locating prey, mates, and shelter. Multisensory systems that control motor behavior even appear
20 in unicellular eukaryotes, such as *Chlamydomonas*, which are important laboratory models for
21 sensory biology. However, we know of no unicellular opisthokont models that control motor
22 behavior using a multimodal sensory suite. Therefore, existing single-celled models for
23 multimodal sensorimotor integration are very distantly related to animals. Here, we describe a
24 multisensory system that controls the motor function of unicellular, fungal zoospores. We find
25 zoospores of *Allomyces arbusculus* exhibit both phototaxis and chemotaxis. While swimming,
26 they move towards light and settle on cellulose membranes exuding combinations of amino
27 acids. Furthermore, we report that closely related *Allomyces* species do not share this
28 multisensory system. Instead, each possesses only one of the two modalities present in *A.*
29 *arbusculus*. This diversity of sensory suites within *Allomyces* provides a rare example of a
30 comparative framework that can be used to examine the evolution of sensory suites. The
31 tractability of *Allomyces* and related fungi as laboratory organisms will allow detailed
32 mechanistic investigations into how sensory systems may have functioned in early opisthokonts
33 before multicellularity allowed for the evolution of specialized cell types.

35 **Introduction**

36 All organisms rely on sensory systems to gather information about their surroundings
37 from external stimuli. The integration of individual sensory modalities into multisensory
38 systems, or sensory suites, greatly increases the amount of information an organism can use to
39 form responses and behaviors. Although multimodal sensory systems are common in
40 multicellular, motile organisms, there are significantly fewer multisensory systems known from
41 unicellular eukaryotes (Govorunova and Sineshchekov, 2005). The relative rarity of these
42 systems in unicellular, laboratory-tractable organisms has resulted in a significant taxonomic gap
43 between current model systems and animals.

44 To address this deficit, we focused on fungi characterized in part by motile, zoosporic life
45 stages. Zoosporic fungi collectively form a clade within the ‘early-diverging lineages’ of fungi,
46 outside the better known Ascomycota and Basidiomycota. They are largely found in freshwater
47 ecosystems with a global distribution (James et al., 2014). Zoosporic fungi are typically
48 characterized as saprobes, such as *Allomyces*, though parasitic life strategies on both plant and
49 animal hosts do exist (Longcore et al., 1999). Similar to all fungi, colonies of *Allomyces* use
50 mycelia to absorb nutrients and ultimately grow reproductive structures. Unlike most fungi,
51 *Allomyces* produce zoosporangia, terminations of mycelial branches that make, store, and
52 ultimately release a multitude of single-celled, flagellate zoospores (Olson, 1984). When the
53 appropriate environmental cues are present, zoospores are produced *en masse*, eventually
54 bursting from zoosporangia (James et al., 2014). Once in the water column, the zoospores rely on
55 a single, posterior flagellum to propel themselves away from the parent colony and towards
56 suitable substrates or hosts (Olson, 1984).

57 During dispersal of the zoosporic life stage, interpretation of environmental cues is
58 critical for the survival and success of the future colony. Zoospores have a finite amount of
59 endogenous energy reserves, and no zoospore is known to metabolize energy from external
60 sources (Suberkropp and Cantino, 1973). This energetic constraint places significant pressure on
61 the zoospore to efficiently locate a favorable environment for settlement and growth. The
62 evolution and maintenance of a sensory system within the unicellular zoospore allows it to
63 evaluate external conditions, move towards suitable habitats, and avoid hazards (James et al.,
64 2014). Previous studies across zoosporic fungi have led to the discovery of a number of sensory
65 modalities that guide zoospore dispersal including chemotaxis, phototaxis, and electrotaxis
66 (Machlis, 1969; Morris et al., 1992; Robertson, 1972). However, these studies have neither tested
67 a single species for multiple sensory modalities, nor posited the possibility that these single
68 senses may only be a portion of a more complex sensorimotor system guiding zoospores.

69 In the fungus *Allomyces*, zoospores use chemotaxis or phototaxis to guide dispersal and
70 settlement (Pommerville and Olson, 1987; Robertson, 1972). Chemotaxis towards the source of
71 amino acid gradients allows zoospores to congregate at the site of an injury or on decaying
72 material in the water column (Machlis, 1969). *Allomyces macrogynus* zoospores possess refined
73 chemosensation, settling on substrates at varied rates in response to different amino acids
74 (Machlis, 1969). Alternatively, the zoospores of *Allomyces reticulatus* display positive

75 phototaxis, potentially leading spores to swim towards the air-water interface (Robertson, 1972).
76 Studies to date have not tested for the presence of chemotaxis in *A. reticulatus* or phototaxis in *A.*
77 *macrogynus*. In animals, positive phototaxis and subsequent ‘rafting’ on floating debris work to
78 considerably increase the dispersal range of planktonic larvae (Epifanio et al., 1989). Similarly,
79 spores attracted to the surface may encounter floating debris, algal hosts, or currents that aid their
80 dispersal.

81 While little is known about the molecular mechanisms of chemotaxis in fungal
82 zoospores, the underpinnings of their photosensitivity are beginning to come to light. The protein
83 responsible for light-detection in zoospores of *Blastocladiella emersonii*, a close relative of
84 *Allomyces*, is a bacteriorhodopsin gene called *CyclOps (Beme-Cycl)* (Avelar et al., 2014). Unlike
85 many bacteriorhodopsins that regulate ion channels, *Beme-Cycl* acts through regulating
86 intracellular cGMP (Avelar et al., 2015). A *CyclOps* gene is present in the genome of *A.*
87 *macrogynus (Amag-Cycl)*, a species that has been anecdotally described as having phototactic
88 zoospores (Olson, 1984). A recent study by Gao et. al., 2015, however, contradicts claims of
89 phototaxis in *A. macrogynus* by revealing the proteins encoded by *Amag-Cycl* are orders of
90 magnitude less sensitive to dark/light transitions than *Beme-Cycl* proteins (Gao et al., 2015). This
91 raises questions about the sensitivity of *CyclOps* proteins needed for phototaxis and mutations
92 potentially responsible for shifts in photosensitivity.

93 The uncertainty surrounding the sensory suites of *Allomyces* zoospores demands
94 experimental evidence to clarify number and types of modalities used during dispersal and
95 settlement. Addressing the current deficits in our understanding of fungal sensory systems is also
96 motivated by the potential to discover a system that will further our knowledge of multisensory
97 evolution and function in early opisthokonts. Here, we investigate the responses to chemical and
98 light gradients in three species of *Allomyces*; revealing previously unknown variation in fungal
99 sensory systems, and discovering a novel multisensory system in a zoosporic fungus.

100

101 **Materials and Methods**

102 *Culture conditions*

103 We used *Allomyces arbusculus* str. ATCC 10983, *Allomyces reticulatus* str. California 70 from
104 ATCC (cat. No. 42465), and *A. macrogynus* from the Roberson lab (U of AZ). We kept cultures
105 of *A. macrogynus* and *A. arbusculus* in both solid and liquid media. For solid media, we used

106 (Machlis, 1953) Emerson YSS (HiMedia M773) at half strength. Colonies transferred aseptically
107 in a laminar flow hood every 4 weeks by moving a chunk of mycelia from the leading edge of
108 the colony onto a new plate. For liquid media, we followed the protocol for Machlis' medium B.
109 We inoculated liquid cultures via sterile transfer of sporangia and mycelia into a 125mL
110 Erlenmeyer flask containing 50mL of liquid media and antibiotics (Machlis, 1953) for the first
111 generation. For all subsequent generations kept in liquid culture, we used dilute salts solution to
112 initiate sporulation of the previous generation's colonies. We then added 1 mL of this zoospore-
113 dilute salts solution (referred to a sporulation product from here on) into new liquid media. Both
114 liquid and solid cultures were grown on an orbital shaker at 140rpm and kept at room
115 temperature (~24C). Cultures in liquid media were kept for a maximum of 5 days, and were
116 considered ready for sporulation after 72 hours. Because *A. reticulatus* did not grow well in
117 liquid media, we cultured *A. reticulatus* on full strength Emerson YSS media for no more than 6
118 weeks. Propagation of *A. reticulatus* cultures in solid media was performed identically to the
119 other species.

120

121 *Sporulation conditions*

122 Liquid cultures of *A. macrogynus* and *A. arbusculus* were considered for sporulation after
123 72 hours. We visually inspected colonies under a microscope to confirm the absence of
124 gametangia. Using a stainless steel sterile mesh, we strained the colonies out of growth media
125 and rinsed them 5 times with dilute salts solution to remove the growth media from the colonies.
126 We then placed the rinsed colonies and strainer in a pyrex dish with 10 mL of dilute salts
127 solution and allowed them to sporulate for no more than 90 min. Once either sufficient spore
128 density had been reached (5×10^5 spores mL^{-1} for chemotaxis, 1×10^6 spores mL^{-1} for phototaxis)
129 or 90 minutes had elapsed, the mesh and colonies were lifted out of the dish (Machlis, 1969).
130 Because *A. reticulatus* was only grown on solid media, we took a surface scraping to lift
131 sporangia from the agar and placed it into a pyrex dish with 10 mL dilute salts solution (Saranak
132 and Foster, 1997). If no zoospores were present, we replaced dilute salts solution every 20
133 minutes for the first hour. Sporulation typically occurred within 8 hours, after which the colonies
134 were strained from the dilute salts solution.

135

136 *Phototaxis trials*

137 We conducted phototaxis trials in a custom 1x5x3 cm (WxHxL) plexiglass chamber. We
138 added 10 mL of sporulation product, diluted to 5×10^5 spores mL^{-1} , to the test chamber and
139 allowed the solution 15 minutes in total darkness to dark adapt and randomize spore distribution.
140 After dark adaption, spores were exposed to a white light (USHIO halogen bulb) through a 5 mm
141 diameter fiber optic cable positioned 5 cm from the leading edge of the test chamber. To
142 calibrate the amount and intensity of light, we used a JAZ Oceanoptics light sensor with
143 Spectrasuite v2.0.162. We adjusted the intensity of the light to $1.8\text{-}1.0 \times 10^{13}$ mol of photons cm^{-2}
144 on the edge closest to the light source. Zoospores were exposed to light for 15 minutes, after
145 which we divided the test chamber into 4 sequential sub-chambers (10x25x15mm) using sterile
146 glass slides. This resulted in 4 sub chambers (1, 2, 3, and 4) arranged linearly so that sub
147 chamber 1 was closest to the light source, while subchamber 4 was the farthest away (Fig. S1A).
148 We gently agitated the liquid in each subchamber to homogenize swimming spore distribution
149 and counted spore density in four, 10 μl samples from each subchamber using a hemocytometer.
150 A total of 10 control treatments (no light exposure) and 18 experimental treatments were
151 conducted for each species.

152

153 *Chemotaxis trials*

154 Chemotaxis trials followed the protocol established by Machlis (1969) (Machlis, 1969).
155 The amino acids and combinations thereof we tested were Lysine (K), Leucine (L), Proline (P),
156 L+K, L+P, K+P, L+K+P, and Buffer (50 mmol KH_2PO_4) solution (referred to as ‘treatment
157 solutions’ from here on). All amino acid concentrations were 5×10^{-4} mol. We created a chemical
158 dispersal apparatus by drilling a hole through the lid of a 60x15mm petri dish and inserting a
159 5mm inner diameter glass pipette. We secured dialysis membrane (3500 MWCO) to the tip of
160 the pipette and positioned it 3mm above the bottom of the petri dish (Fig. S1B). This creates a
161 gradient in the petri dish of whatever solution is placed behind the dialysis membrane, allowing
162 zoospores to navigate to the membrane, where they settle and can later be counted. The dialysis
163 membrane was soaked and rinsed with DI water for 24 hours to remove potential contaminants
164 and bubbles that would affect results (Carlile and Machlis, 1965).

165 To test for chemotaxis, we added 10 mL of sporulation product (diluted to 5×10^4 spores
166 mL^{-1}) to the petri dish and 300 μl of treatment solution into the pipette. As a control, we used
167 300 μl of buffer alone. We allowed the spores to react to the gradient in total darkness for 90

168 minutes. At the end of the trial time, we removed the pipette and dialysis membrane from the
169 dish and gently shook it to remove excess liquid (Machlis, 1969). We counted spores settled on
170 the membrane under an Olympus szx7 at 400x or greater magnification.

171

172 *Molecular Methods:*

173 A) PCR, cDNA synthesis & sequencing: Because genomic data existed for *A. macrogynus* but
174 expression data did not, we used PCR to attempt to identify if *CyclOps* genes are expressed in *A.*
175 *macrogynus* zoospores. mRNA was extracted from zoospores using a NucleoSpin RNA XS kit.
176 We synthesized cDNA using the Clontech cDNA synthesis kit. Primers were designed from
177 putative rhodopsin/guananyl-cyclase fusion proteins identified from the BROAD institute's
178 *Allomyces macrogynus* genome, using the *CyclOps* protein sequence from *Blastocladiella*
179 *emersonii* as bait sequences (Avelar et al., 2014). Sets of primers were designed in IDT
180 PrimerQuest. All PCR products were visualized using a 1% agarose gel with 100bp ladder. PCR
181 for *CyclOps* was only done on *A. macrogynus* as transcriptomes for *A. reticulatus* and *A.*
182 *arbusculus* would yield expression data.

183 RNA was isolated from zoospores of *A. reticulatus* and *A. arbusculus* using Nucleospin xsRNA
184 kit, and cDNA was synthesized using the NEBNext RNA First and Second Strand Synthesis
185 modules. cDNA was sequenced using a multiplexed Illumina HiSeq lane at approximately 50x
186 coverage.

187 B) Bioinformatics and Statistics: We trimmed Illumina data using Trimmomatic (Bolger et al.,
188 2014), assembled using Trinity 2.0, and analyzed on the UCSB Osiris bioinformatics platform
189 (Giardine et al., 2005; Oakley et al., 2014). Putative *CyclOps* proteins were identified using
190 *Beme-Cycl* as a bait sequence in BLASTn searches against the *A. macrogynus* genome, NCBI
191 bioproject 20563, and the new *A. reticulatus* and *A. arbusculus* zoospore transcriptomes. Any
192 sequence with an e-score lower than $1e-40$ was considered as a candidate. We then used the 'get
193 orf' feature from Trinity to produce predicted proteins from candidate genes, selecting the
194 longest orfs with the highest similarity to *Beme-Cycl* protein when reciprocally BLASTed using
195 blastp. We identified the putative *CyclOps* gene in both *A. reticulatus* and *A. arbusculus* (*Aarb-*
196 *Cycl*). Reads from *A. arbusculus* transcriptome were mapped back to the putative *Aarb-Cycl*
197 using Bowtie2 (Langmead and Salzberg, 2012) and visualized using IGV viewer
198 (Thorvaldsdóttir et al., 2013). Because the bacteriorhodopsin and guanylate-cyclase domains

199 appeared in different ORFs on the same strand, each base was manually examined for
200 uncertainty and low support. A guanine at site 378 was manually removed due to low coverage
201 and low support in the reads, implying that the addition of guanine at position 378 most likely an
202 assembly artifact. The manually edited *Aarb-Cycl* gene produced a single predicted orf with the
203 appropriate bacteriorhodopsin-guanlyl cyclase domains (Fig. S2).

204 Candidate proteins were aligned using MAFFT under the L-INS-i strategy. Outgroups
205 were selected based on a previous analysis (Porter et al., 2011) (Fig. S2). The alignment was
206 used to create a phylogeny of candidate genes with RAxML 8 (Stamatakis, 2014) and 100
207 bootstrap replicates using the GTR + Γ model. Trees were visualized in Evolview (He et al.,
208 2016) and annotations were added in Adobe Illustrator.

209 Comparisons of zoospore phototaxis behavior were analyzed using JMP v12.0. Average
210 spore counts per subchamber per trial were analyzed using pairwise Tukey's HSD between
211 control and experimental sub-chambers. Although sample size was low, each sample is an
212 average of four replicates - making effective sample size close to 40 for each treatment.
213 Zoospore chemotaxis was analyzed using Wilcoxon each pair due to the nonparametric
214 distribution of results and small sample size (n=10).

215

216 **Results**

217 *A. reticulatus* relies on phototaxis

218 Zoospores of *A. reticulatus* showed no significant deviation from the control when
219 exposed to any amino acid treatment ($P > 0.05$ for all treatments) (Fig. 1). In accordance with
220 existing literature, *A. reticulatus* showed a significant response to a light gradient (Robertson,
221 1972). The number of zoospores swimming in the subchamber closest to the light source (Fig. 2)
222 was significantly higher than when no light source was present ($P = 0.0005$).

223

224 *A. macrogynus* relies on chemotaxis

225 As seen in previous experiments, *A. macrogynus* zoospores displayed a significant
226 response to all amino acid treatments compared to the control (Machlis, 1969). Proline ($P =$
227 0.0294), leucine ($P=0.0275$), lysine ($P=0.0294$), and any combination of two or three amino
228 acids when compared to a control ($P < 0.001$) (Fig. 1). Zoospore response to increasing treatment
229 complexity was non-linear though roughly equal for all unique combinations of equal

230 complexity. *A. macrogynus* zoospores showed no response when exposed to a light gradient (Fig.
231 2). The number of zoospores in all sub-chambers were the same for both light and dark trials (P
232 = 0.9976).

233

234 *Allomyces arbusculus uses both chemotaxis and phototaxis in a multisensory system*

235 As expected from existing literature, *A. arbusculus* zoospores responded similarly to the
236 zoospores of *A. macrogynus* when exposed to amino acid treatments. The number of spores
237 settled increased in a nonlinear fashion as the complexity of the treatment increased, though at a
238 lower average number of settled spores when compared to *A. macrogynus*: K+P ($P = 0.0014$),
239 K+L ($P = 0.0014$), L+P ($P = 0.0008$), K+L+P ($P = 0.0004$) (Fig. 1). As opposed to *A.*
240 *macrogynus*, *A. arbusculus* does not respond to, or cannot detect, gradients of single amino acids
241 ($P > 0.05$ for all single A.A. treatments) with the possible exception of Proline. We found that no
242 zoospores settled when *A. arbusculus* was exposed to trials of Proline alone, potentially
243 indicating the potential for negative chemotaxis or inhibition of settlement in response to
244 gradients of Proline by itself. However, we can not definitively resolve this reaction with our
245 sample size (Proline v. Control: $P = 0.072$; $N=10$). When exposed to a directional light source, *A.*
246 *arbusculus* display positive phototaxis (Fig. 2). The number of zoospores in the sub-chamber
247 closest to the light was significantly higher ($P < 0.0001$) in light vs. dark trials and was
248 comparable to the response of *A. reticulatus* zoospores.

249

250 *CyclOps is present in all species, may not be expressed in A. macrogynus zoospores*

251 Phylogenetic analysis of putative *CyclOps* genes reveals *CyclOps* presence in all three
252 samples (*A. arbusculus* & *A. reticulatus*: transcriptome data. *A. macrogynus*: previously
253 available genome data). The single copy of *CyclOps* recovered from the *A. arbusculus*
254 transcriptome revealed a possible truncation of the Guanylyl cyclase domain (Fig. 3). Both *Aarb-*
255 *Cycl* and *Amag-Cycl* share a mutation at the putative functional residue F313 to I313. Despite the
256 success of positive controls indicating successful PCR amplification, no primers successfully
257 amplified *Amag-Cycl* from *A. macrogynus* zoospores.

258

259 Discussion

260 Understanding how sensory modalities evolve and integrate with other behavioral circuits
261 remains an open question in neurobiology and evolutionary biology. The *Allomyces* genus, with
262 new variation in sensory suites discovered in this study, will aid in answering these questions.
263 Previous studies had shown *Allomyces* spores use either chemotaxis or phototaxis to guide
264 dispersal. Here, we reveal that the sensorimotor system in *A. arbusculus* is multimodal - able to
265 process both chemical and light cues. Additionally, our results reveal the previously unknown
266 complexity and variation of sensorimotor systems in *Allomyces*.

267

268 *Variation in sensory modalities across Allomyces:*

269 In this report, we discover unknown variation in the distribution of sensory modalities
270 across the genus. This variation manifests in two ways: the types of sensory modalities used by
271 each species of *Allomyces* and the responses of *A. arbusculus* and *A. macrogynus* zoospores to
272 the same amino acids. The lack of phototaxis, coupled with the inability to amplify *CyclOps*
273 from zoospore mRNA in *A. macrogynus* is quite interesting due to conflicting reports between
274 previous studies. These studies conflictingly report that *A. macrogynus* zoospores are either
275 phototactic (through anecdotal evidence) (Olson, 1984) or that the photosensitive protein, Amag-
276 Cycl, does not respond effectively to light (Gao et al., 2015). Our findings support the hypothesis
277 that *CyclOps* in *A. macrogynus* no longer effectively differentiates between light and dark, and
278 suggest that *CyclOps* expression has been lost in zoospores. With the loss of phototaxis, the
279 distribution and settlement of *A. macrogynus* zoospores likely deviated greatly from both *A.*
280 *reticulatus* and *A. arbusculus* in natural settings.

281 The variation in *Allomyces* sensory suites discovered in this study coupled with the
282 convergent function of *CyclOps* and animal opsins make it critical to our understanding of the
283 evolutionary history of light sensing. Animal photoreception, mediated through Type II opsins,
284 operates through intracellular regulation of cyclic nucleotides. Non-animal photoreception,
285 mediated through Type I opsins, operates through channel and sensory rhodopsins (SRII). SRIIs,
286 like type II opsins, induce a signal transduction cascade. However, unlike animal opsins, SRIIs
287 do not regulate cyclic nucleotide concentrations. Instead, SRIIs indirectly regulate CheY, a
288 protein that controls flagellar motion (Klare et al., 2004). Type I and II opsins are considered a
289 spectacular example of convergent evolution (Larusso et al., 2008). *CyclOps* represents a third

290 case of convergence, where protein function may modulate intracellular cGMP levels, yet the
291 sequence similarity of *CyclOps* imply its origin as a diversification of type I opsins (Avelar et al.,
292 2015). Studying the evolution of *CyclOps* sequence function through the variation in *Allomyces*
293 will yield further insights into the evolution of novel photosensory mechanisms.

294 The lack of chemotaxis in *A. reticulatus* highlights the variation in *Allomyces* sensory
295 system evolution. While previous studies uncovered differences in the combinations of amino
296 acids *A. arbusculus* and *A. macrogynus* zoospores prefer (Machlis, 1969), no one tested the
297 possibility of a complete lack of chemotaxis in a close relative. The discovery of *A. reticulatus*'s
298 lack of chemotaxis reveals a turnover in sensory modalities responsible for controlling a vital
299 behavior across the genus. Future studies will use the variation in both chemotaxis and
300 phototaxis across *Allomyces* as a platform to understand behavioral integration, multisensory
301 evolution, and sensory remodeling in an organism closely resembling ancestral opisthokonts.

302

303 *The Multisensory System of Allomyces arbusculus:*

304 *Allomyces arbusculus* zoospores present an easily culturable, laboratory tractable system
305 for investigating multimodal sensation in unicellular systems and its underlying mechanisms.
306 Previous studies have independently confirmed that zoospores use a diversity of senses, but most
307 zoospores have only been tested for a single sense (Avelar et al., 2014; Machlis, 1969; Morris et
308 al., 1992; Robertson, 1972). Our findings represent the first study of zoospore multisensory
309 capabilities, and a concrete example of multimodal sensorimotor control in a unicellular
310 opisthokont (Fig. 1-2). Though choanoflagellates fall within Opisthokonta (Cavalier-Smith et al.,
311 2014) and potentially exhibit both areo- and pH-taxis, it remains unknown if the sensory
312 modalities in colonies (areotaxis) are also used to direct the dispersal stage (pH-taxis)
313 (Kirkegaard et al., 2016; Miño et al., 2017).

314 Zoospores, as unicellular, flagellated cells, might closely represent the ancestral
315 opisthokont phenotype (Cavalier-Smith et al., 2014). Specialized cell types and functions may
316 often evolve through subfunctionalization followed by elaboration of the ancestral cell's
317 functions (Arendt et al., 2016). This implies that as multicellular opisthokonts evolved, the
318 foundation for specialized sensory modalities already existed. Under the subfunctionalization
319 hypothesis, multimodal systems in unicellular organisms, such as we report in *A. arbusculus*,
320 must have evolved prior to subfunctionalization in ancestral, multicellular opisthokonts. Future

321 studies of the multimodal sensorimotor system in *A. arbusculus* zoospores and the variation in
322 modalities across *Allomyces* may uncover how multiple senses became integrated into behavioral
323 responses in ancestral opisthokonts. Understanding these mechanisms in the context of the
324 cellular subfunctionalization hypothesis will further our understanding of sensorimotor
325 evolution, elaboration and individuation through cellular specialization.

326

327 *Conclusions*

328 We present a multimodal sensorimotor system in a unicellular life stage of a fungus. The
329 multisensory suite of *A. arbusculus* zoospores is an excellent system to study how sensory
330 modalities integrate into existing behavioral regimes. Together with existing models of
331 unicellular sensory mechanisms, the variation in sensory modalities in *Allomyces* and other early
332 diverging fungi will allow us to formulate more accurate conclusions about the evolution of
333 complex sensory suites and multisensory systems in ancestral eukaryotes. Lastly, the relatively
334 narrow taxonomic breadth associated with the multiple transitions in sensory suites during
335 *Allomyces* evolution will allow testing of broad questions in evolution; such as the role
336 multimodal cell types play in the origin and evolution of specialized traits, and how emergent
337 behaviors evolve during sensory remodeling.

338

339

340

341 **Acknowledgements**

342 The authors would like to thank Robert Roberson for supplying *A. macrogynus* and Jason Stajich
343 for his advice and guidance on molecular work in fungus systems. Additionally, the authors
344 would like to thank Oren Malvey for his help in maintaining cultures.

345

346 **Competing interests**

347 The authors declare no conflict of interests.

348

349 **Author Contributions**

350 A.S. and T.O. designed experiments. A.S. carried out experiments and analyzed data. A.S. and
351 T.O. wrote and edited the manuscript.

352

353 **Funding**

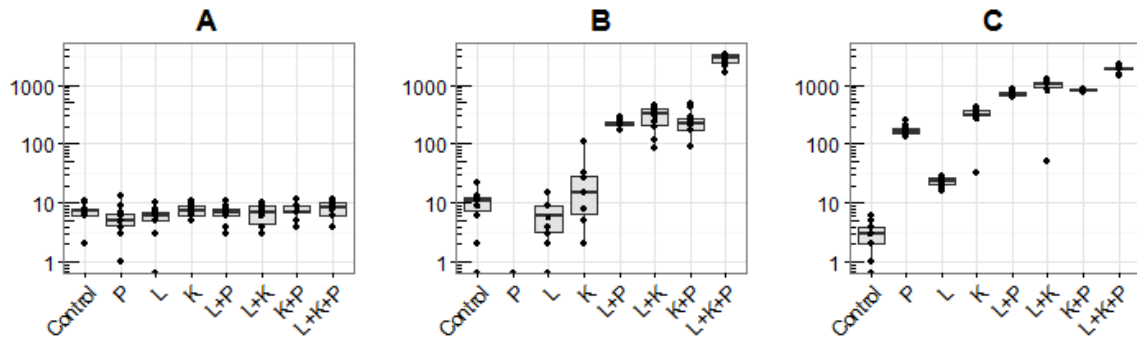
354 This work was supported by a Sigma-Xi Grant In Aid of Research and Rosemary Grant Award
355 awarded to A.S. and NSF #1456859 awarded to T.O.

356

357 **Data Availability**

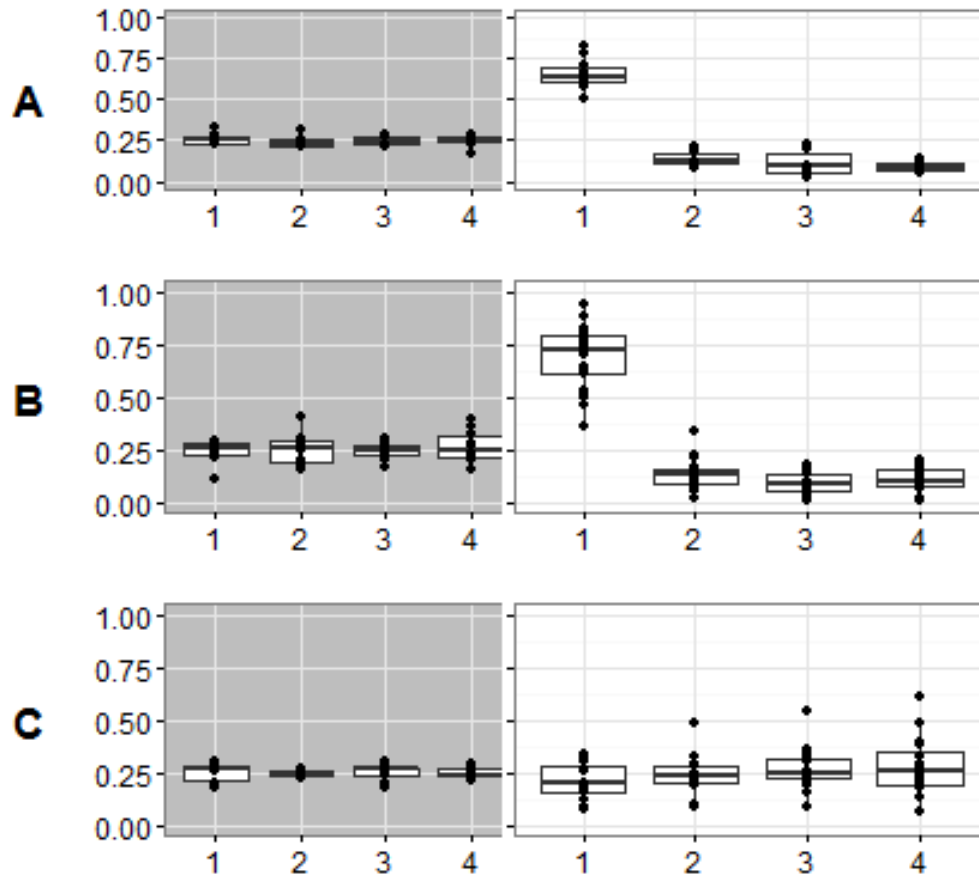
358 Alignment, newick, and behavioral data collected for this study is available for download at
359 https://bitbucket.org/swafford/multisensory_systems_JEB_2017.

360



361
362 **Figure 1. The number of zoospores settled on the dialysis membrane in response to varying**
363 **amino acid treatments. (A) *Allomyces reticulatus*, (B) *A. arbusculus*, (C) *A. macrogynus*.** Each
364 column represents the number of zoospores settled on 2mm² dialysis membrane after 90 minutes.
365 Squares represent means. **Control**, Proline (**P**), Leucine (**L**), Lysine (**K**), and combinations
366 thereof. N=10 for all treatments, Y axis in log scale.
367

368

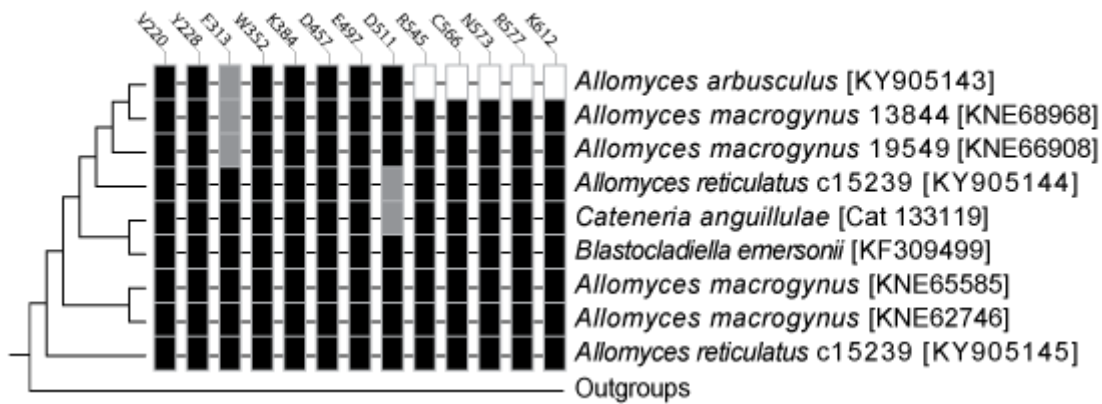


369

370 **Figure 2. The distribution of swimming zoospores found in each subchamber in phototaxis**
371 **trials, shown as percentage. (A) *A. reticulatus* (B) *A. arbusculus* or (C) *A. macrogynus***
372 **zoospore distribution after 30 minutes of darkness (grey background) or 15 minutes of darkness**
373 **followed by 15 minutes exposure to directional light (white background). The directional light**
374 **source was positioned so light intensity was strongest in sub-chamber 1 and lowest in sub-**
375 **chamber 4.**

376

377



379

380 **Figure 3. Cladogram showing the relationships and conserved amino acid residues in**
381 **CyclOps proteins.** Boxes indicate amino acid residues critical for binding (Avelar et al., 2014),
382 with residue numbers based on position in unaligned Beme-Cycl (AIC07007.1). Black boxes
383 indicate an amino acid matching at that residue when compared to Beme-Cycl, grey boxes
384 indicate a mutation, and white boxes indicate a gap.

384

385 **References**

- 386 **Arendt, D., Musser, J. M., Baker, C. V. H., Bergman, A., Cepko, C., Erwin, D. H., Pavlicev,**
387 **M., Schlosser, G., Widder, S., Laubichler, M. D., et al.** (2016). The origin and evolution
388 of cell types. *Nat. Rev. Genet.* **17**, 744–757.
- 389 **Avelar, G. M., Schumacher, R. I., Zaini, P. A., Leonard, G., Richards, T. A. and Gomes, S.**
390 **L.** (2014). A rhodopsin-guanylyl cyclase gene fusion functions in visual perception in a
391 fungus. *Curr. Biol.* **24**, 1234–1240.
- 392 **Avelar, G. M., Glaser, T., Leonard, G., Richards, T. A., Ulrich, H. and Gomes, S. L.** (2015).
393 A Cyclic GMP-Dependent K⁺ Channel in the Blastocladiomycete Fungus *Blastocladiella*
394 *emersonii*. *Eukaryot. Cell* **14**, 958–963.
- 395 **Bolger, A. M., Lohse, M. and Usadel, B.** (2014). Trimmomatic: a flexible trimmer for Illumina
396 sequence data. *Bioinformatics* **30**, 2114–2120.
- 397 **Carlile, M. J. and Machlis, L.** (1965). A Comparative Study of the Chemotaxis of the Motile
398 Phases of Allomyces. *Am. J. Bot.* **52**, 484–486.
- 399 **Cavalier-Smith, T., Chao, E. E., Snell, E. A., Berney, C., Fiore-Donno, A. M. and Lewis, R.**
400 (2014). Multigene eukaryote phylogeny reveals the likely protozoan ancestors of
401 opisthokonts (animals, fungi, choanozoans) and Amoebozoa. *Mol. Phylogenet. Evol.* **81**,
402 71–85.
- 403 **Epifanio, C. E., Masse, A. K. and Garvine, R. W.** (1989). Transport of blue crab larvae by
404 surface currents off Delaware Bay, USA. *Marine ecology progress series. Oldendorf* **54**,
405 35–41.
- 406 **Gao, S., Nagpal, J., Schneider, M. W., Kozjak-Pavlovic, V., Nagel, G. and Gottschalk, A.**
407 (2015). Optogenetic manipulation of cGMP in cells and animals by the tightly light-
408 regulated guanylyl-cyclase opsin CyclOp. *Nat. Commun.* **6**, 8046.
- 409 **Giardine, B., Riemer, C., Hardison, R. C., Burhans, R., Elnitski, L., Shah, P., Zhang, Y.,**
410 **Blankenberg, D., Albert, I., Taylor, J., et al.** (2005). Galaxy: a platform for interactive
411 large-scale genome analysis. *Genome Res.* **15**, 1451–1455.
- 412 **Govorunova, E. G. and Sineshchekov, O. A.** (2005). Chemotaxis in the green flagellate alga
413 *Chlamydomonas*. *Biochemistry* **70**, 717–725.
- 414 **He, Z., Zhang, H., Gao, S., Lercher, M. J., Chen, W.-H. and Hu, S.** (2016). Evolvview v2: an
415 online visualization and management tool for customized and annotated phylogenetic trees.
416 *Nucleic Acids Res.* **44**, W236–41.
- 417 **James, T. Y., Porter, T. M. and Wallace Martin, W.** (2014). 7 Blastocladiomycota. In
418 *Systematics and Evolution*, pp. 177–207. Springer Berlin Heidelberg.
- 419 **Kirkegaard, J. B., Bouillant, A., Marron, A. O., Leptos, K. C. and Goldstein, R. E.** (2016).

- 420 Aerotaxis in the closest relatives of animals. *Elife* **5**,.
- 421 **Klare, J. P., Gordeliy, V. I., Labahn, J., Büldt, G., Steinhoff, H.-J. and Engelhard, M.**
422 (2004). The archaeal sensory rhodopsin II/transducer complex: a model for transmembrane
423 signal transfer. *FEBS Lett.* **564**, 219–224.
- 424 **Langmead, B. and Salzberg, S. L.** (2012). Fast gapped-read alignment with Bowtie 2. *Nat.*
425 *Methods* **9**, 357–359.
- 426 **Larusso, N. D., Ruttenberg, B. E., Singh, A. K. and Oakley, T. H.** (2008). Type II opsins:
427 evolutionary origin by internal domain duplication? *J. Mol. Evol.* **66**, 417–423.
- 428 **Longcore, J. E., Pessier, A. P. and Nichols, D. K.** (1999). Batrachochytrium Dendrobatidis
429 gen. et sp. nov., a Chytrid Pathogenic to Amphibians. *Mycologia* **91**, 219–227.
- 430 **Machlis, L.** (1953). Growth and Nutrition of Water Molds in the Subgenus Euallomyces. II.
431 Optimal Composition of the Minimal Medium. *Am. J. Bot.* **40**, 450–460.
- 432 **Machlis, L.** (1969). Zoospore Chemotaxis in the Watermold Allomyces. *Physiol. Plant.* **22**,
433 126–139.
- 434 **Miño, G. L., Koehl, M. A. R., King, N. and Stocker, R.** (2017). Finding patches in a
435 heterogeneous aquatic environment: pH-taxis by the dispersal stage of choanoflagellates.
436 *Limnol. Oceanogr.* **2**, 37–46.
- 437 **Morris, B. M., Reid, B. and Gow, N. A. R.** (1992). Electrotaxis of zoospores of Phytophthora
438 palmivora at physiologically relevant field strengths. *Plant Cell Environ.* **15**, 645–653.
- 439 **Oakley, T. H., Alexandrou, M. A., Ngo, R., Pankey, M. S., Churchill, C. K., Chen, W. and**
440 **Lopker, K. B.** (2014). Osiris: accessible and reproducible phylogenetic and phylogenomic
441 analyses within the Galaxy workflow management system. *BMC Bioinformatics* **15**, 230.
- 442 **Olson, L. W.** (1984). *Allomyces: A Different Fungus*. Council for Nordic Publications in Botany.
- 443 **Pommerville, J. C. and Olson, L. W.** (1987). Negative Chemotaxis of Gametes and Zoospores
444 of Allomyces. *Microbiology* **133**, 2573–2579.
- 445 **Porter, T. M., Martin, W., James, T. Y., Longcore, J. E., Gleason, F. H., Adler, P. H.,**
446 **Letcher, P. M. and Vilgalys, R.** (2011). Molecular phylogeny of the Blastocladiomycota
447 (Fungi) based on nuclear ribosomal DNA. *Fungal Biol.* **115**, 381–392.
- 448 **Robertson, J. A.** (1972). Phototaxis in a new Allomyces. *Arch. Mikrobiol.* **85**, 259–266.
- 449 **Saranak, J. and Foster, K.** (1997). Rhodopsin guides fungal phototaxis. *Nature*.
- 450 **Stamatakis, A.** (2014). RAxML version 8: a tool for phylogenetic analysis and post-analysis of
451 large phylogenies. *Bioinformatics* **30**, 1312–1313.
- 452 **Suberkropp, K. F. and Cantino, E. C.** (1973). Utilization of endogenous reserves by

- 453 swimming zoospores of *Blastocladiella emersonii*. *Arch. Mikrobiol.* **89**, 205–221.
- 454 **Thorvaldsdóttir, H., Robinson, J. T. and Mesirov, J. P.** (2013). Integrative Genomics Viewer
455 (IGV): high-performance genomics data visualization and exploration. *Brief. Bioinform.* **14**,
456 178–192.
- 457